

## INFRARED STUDIES OF EPSILON AURIGAE IN ECLIPSE

Robert E. Stencel, Brian K. Kloppenborg and Randall E. Wall, Jr.

*Dept. Physics & Astronomy, University of Denver, Denver CO 80208 USA.*

Jeffrey L. Hopkins

*Hopkins Phoenix Observatory, Phoenix, AZ 85033 USA.*

Steve B. Howell

*National Optical Astronomy Observatories, Tucson, AZ 85719 USA.*

D. W. Hoard

*Spitzer Science Center, California Institute of Technology, Pasadena, CA 91125 USA.*

John Rayner, Schelte Bus and Alan Tokunaga

*Institute for Astronomy, University of Hawaii, 2680 Woodlawn Dr., Honolulu, HI 96822, USA.*

Michael L. Sitko and Suellen Bradford, Esq.

*Dept. Physics, Cincinnati University, Cincinnati OH USA and  
Space Science Institute, Boulder CO, USA*

Ray W. Russell and David K. Lynch

*The Aerospace Corporation, Los Angeles, CA 90009 USA.*

Heidi Hammel and Barbara Whitney

*Space Science Institute, 4750 Walnut Street, Suite 205, Boulder, CO 80301 USA.*

Glenn Orton and Padma Yanamandra-Fisher

*Jet Propulsion Laboratory, California Institute of Technology, Pasadena, CA 91109, USA.*

Joseph L. Hora

*Harvard-Smithsonian Center for Astrophysics, 60 Garden St., Cambridge, MA 02138, USA.*

Philip Hinz, William Hoffmann and Andrew Skemer

*Steward Observatory, Department of Astronomy, University of Arizona, Tucson, AZ 85721 USA.*

Email inquiries: [rstencel@du.edu](mailto:rstencel@du.edu); Accepted Sept.2011 for the Astronomical  
Journal

## ABSTRACT

We report here on a series of medium resolution spectro-photometric observations of the enigmatic long period eclipsing binary epsilon Aurigae, during its eclipse interval 2009-2011, using near-infrared spectra obtained with SpeX on IRTF, mid-infrared spectra obtained with BASS on AOES and IRTF, MIRSI on IRTF and MIRAC4 on MMT, along with mid-infrared photometry using MIRSI on IRTF and MIRAC4 on MMT, plus 1995-2000 timeframe published photometry and data obtained with Denver’s TNTCAM2 at WIRO. The goals of these observations included: (1) comparing eclipse depths with prior eclipse data, (2) confirming the re-appearance of CO absorption bands at and after mid-eclipse, associated with sublimation in the disk, (3) seeking evidence for any mid-infrared solid state spectral features from particles in the disk, and (4) providing evidence that the externally-irradiated disk has azimuthal temperature differences. IR eclipse depths appear similar to that observed during the most recent (1983) eclipse, although evidence for post-mid-eclipse disk temperature increase is present, due to F star heated portions of the disk coming into view. Molecular CO absorption returned 57 days after nominal mid-eclipse, but was not detected at mid-eclipse plus 34 days, narrowing the association with differentially heated sub-regions in the disk. Transient He I 10830A absorption was detected at mid-eclipse, persisting for at least 90 days thereafter, providing a diagnostic for the hot central region. The lack of solid-state features in Spitzer IRS, BASS and MIRAC spectra to date suggests the dominance of large particles (micron-sized) in the disk. Based on these observations, mid-infrared studies out of eclipse can directly monitor and map the disk thermal changes, and better constrain disk opacity and thermal conductivity.

*Subject headings:* binaries: eclipsing - stars: individual: epsilon Aurigae - protoplanetary disks

## 1. Introduction

The bright eclipsing binary star, epsilon Aurigae, has long fascinated astronomers because they could determine the nature of one star in the system, but not the other (for a review, see Guinan and Dewarf, 2002). The crux of the problem was that the early F type star in this single-lined spectroscopic binary resembles a supergiant and thus should have a comparably massive companion ( $\sim 10$  to  $15M_{\odot}$ ). However, the companion is vastly underluminous for the inferred mass. Various models have been proposed, but one model involves a post-AGB F star and a fairly normal upper main sequence star surrounded by disk of obscuring material (Huang, 1965; Lambert and Sawyer, 1986). Evidence for the existence of this disk was first provided by Backman et al. (1984, 1985), who detected the infrared presence of an extended, 500K source in the system. Predictions of azimuthal asymmetry in disk structure, due to external heating by the F star, have been provided

by Takeuti (1986, 2011). Interferometric H band imaging during the start of the current eclipse has confirmed the existence of the disk and provided strong constraints on its dimensions and the system mass ratio (Kloppenborg et al. 2010, hereafter KSM). These considerations and more set the stage for confirmation and extension of prior results, given this first eclipse of the 21st century (see Stencel, 2010).

### 1.1. IR Light Curves

We are fortunate to have well determined optical light curves, due to the International Campaign organized by Jeffrey Hopkins (Hopkins and Stencel, 2011), which has provided thousands of UBVRJH measurements since 2006, and earlier. From these data, times of contact have been established as: First = RJD 55,060 ( $V \sim 3.00$ ); Second = RJD 55,200 ( $V \sim 3.80$ ); Mid-eclipse circa RJD  $55,390 \pm 10$  days ( $V \sim 3.75$ ). RJD = J.D. minus 2,400,000, and here we denote *Second* and *Third* contacts as reference points, even though the non-circular disk causing the eclipse will not produce a sharp second or third contact in the traditional eclipsing binary star sense. Observed times of egress were: *Third* = RJD 55,620 ( $V \sim 3.80$ ) and *Fourth* = RJD 55,720 ( $V \sim 3.1$ ). Note that egress also featured a pronounced change of slope starting at RJD 55,360 ( $V \sim 3.3$ ). The persistence of out of eclipse variations during totality adds some uncertainty as well, but we adopt the foregoing times of contact for use in the discussion that follows, anticipating that small refinements will be forthcoming, as part of post-eclipse analyses.

A re-analysis of the Spectral Energy Distribution (SED) by Hoard, Howell and Stencel (2010, hereafter HHS) shows a transition between F star (7500K) and the cold disk ( $550 \pm 50$ K during total eclipse phase) at/near  $3 \mu\text{m}$ . The combined effects of eclipse attenuation of the F star, and the predicted temperature rise as heated portions of the disk come into view after mid-eclipse (Takeuti 1986, 2011), both should result in measureable changes to the SED at near and mid-IR wavelengths. The first effect was exploited by Backman et al. (1984) during the last eclipse, and they thus discovered the 550K disk signature, using 2 to  $20 \mu\text{m}$  wavelength-dependent eclipse depths, with Capella as the primary calibration star. However, their published monitoring only covered the first half of the long eclipse, and did not address the second effect, the externally-heated disk that comes increasingly into view after mid-eclipse. In this paper, we seek to measure and quantify both effects.

### 1.2. Spectral Line Changes: CO, and He I

During the previous eclipse in 1983, Hinkle & Simon (1987) collected high resolution, K band FTS data that showed a strong asymmetry in the strength of molecular CO (2-0) spectral features in the near-infrared ( $2.29 \mu\text{m}$ ), appearing only *after* mid-eclipse, and persisting well past optical fourth contact (the nominal end of eclipse). They described the CO column density as being at

least 80 times larger in the trailing edge of the disk compared to the leading edge, with excitation temperature rising to  $1000 \pm 150\text{K}$ , and column densities reaching  $3 \times 10^{20} \text{ CO cm}^{-2}$ . From velocity measurements and for Keplerian rotation, they constrained component masses to be 4 - 7  $M_{\odot}$  for the F star, and 7 - 10  $M_{\odot}$  for the disk and its central object. This is consistent with the 2:3 mass ratio deduced interferometrically (KSM). It also is comparable to the 6  $M_{\odot}$  central star of the disk, inferred from the SED (HHS), as well as the 3 to 6  $M_{\odot}$  for the central star inside the disk, and less than 3 $M_{\odot}$  for the F star, deduced by Lambert and Sawyer (1986) based on velocities derived from the optically thin K I 7699A line. Hinkle and Simon also reported a large enhancement in the  $^{13}\text{C}$  abundance in the disk gas, indicating nuclear processing has occurred in the assumed source, the F star, implying that it is an evolved object. In this paper, we confirm the re-appearance of CO again after mid-eclipse in 2010. Also, as a result of this monitoring, the remarkable He I 10830A line was detected for the first time, appearing strongly in absorption following mid-eclipse (atop a weak photospheric feature previously and subsequently seen). Details are given below.

### 1.3. *Limits on Solid State Features*

Less well constrained is the dust to gas ratio of the disk and its overall mass, in part because there are no dust signatures detected. The infrared spectrum provided by Spitzer IRS presents a largely featureless continuum, implying large particles ( $\geq 0.1 \mu\text{m}$ ). The analogy with appearance of CO suggests the possibility that 10  $\mu\text{m}$  silicates, due to smaller particles, may appear after mid-eclipse due to sublimation by F star heating. In this paper, we report on a series of mid-infrared photometric and spectroscopic observations to investigate this. Defining the dust to gas ratio remains an important goal in the study of this disk and relating it to other transitional disks.

## 2. The Observations

Our observational objectives included monitoring infrared flux levels at multiple wavelengths, exploring spectral line profile changes and especially watching for the predicted re-appearance of molecular CO (2-0) bands near 2.3  $\mu\text{m}$ . Observations upon which this paper is based were obtained with a variety of telescopes and instruments, as detailed below. Photometric and spectroscopic observations were obtained at irregular intervals depending on time allocations, weather and other factors. Optical photometry, spectroscopy, spectro-polarimetry and interferometry were pursued in parallel as part of the overall eclipse campaign, and those results are reported elsewhere.

### 2.1. *The near infrared: IRTF/SpeX*

SpeX is a moderate resolution ( $R \sim 2500$ ), near-IR (1-5  $\mu\text{m}$ ) spectrometer located at the NASA Infrared Telescope Facility (IRTF), as described by Rayner et al. (2003). Observations were

made as early as 2008 and subsequently with increasing frequency, to as often as monthly during the second half of eclipse, in 2010. Routine telluric correction and calibration was accomplished by comparison with simultaneous observations of nearby A0V stars (notably HD30169 and HD29526), using SpeXtool (Cushing et al. 2004; Vacca et al. 2003). Further calibration checks were made in comparison with broadband J and H measurements and slitless BASS data (see below). In Table 1 we list the SpeX observational details, and in Table 2 we list the monochromatic fluxes in  $W m^{-2}$  at selected continuum wavelengths. Individual signal-to-noise based uncertainties formally were less than one percent at the shortest wavelengths, increasing toward longer wavelengths, unless noted otherwise. Absolute calibration is estimated to lie within an uncertainty range of less than 5 percent.

### 2.1.1. Continuum variations

Figure 1 shows SpeX observations during eclipse ingress and totality phases. Corrections for telluric features in the spectra are not perfect, but the overall continuum is substantially decreased during the eclipse. During eclipse, Backman et al. (1984) noted uniform decrease at J, H, K and L bands [ $1.25$ ,  $1.65$ ,  $2.2$  and  $3.80\mu m$  respectively] of  $0.72 \pm 0.03$  magnitudes, then decreasing at M band [ $4.8\mu m$ ] to  $0.66$  magnitudes, at N band [ $10.1\mu m$ ] to  $0.61$  mag, and at Q band [ $20\mu m$ ] to  $0.32 \pm 0.06$  magnitudes. These correspond to flux *ratios* at JHKL of  $0.52$ ; at M:  $0.55$ ; at N:  $0.57$ , and at Q:  $0.74$ , which Backman et al. recognized as the spectral energy dominance of the cold disk affecting the longest wavelength eclipse depth ratios.

Our data appear consistent with these reported eclipse depth ratios. When we compare the monochromatic flux *ratios* between 2009 Sep 10 (first contact) and 2010 Feb 23 (second contact), we find at  $1.1\mu m$ :  $0.56$ ; at  $1.65\mu m$ :  $0.55$ ; at  $2.1\mu m$ :  $0.54$ ; at  $3.15\mu m$ :  $0.51$ ; at  $3.95\mu m$ :  $0.43$ , but then rising at  $4.64\mu m$  to  $0.55$ . Our longest SpeX wavelengths are the most affected by telluric correction. For the shorter wavelengths, these appear consistent with Backman et al., within 3 percent uncertainty. However, if we ratio fluxes between our *pre – eclipse* data (2008 Jan 27) and second contact (2010 Feb 23), we obtain deeper eclipse ratios: at  $1.1\mu m$ :  $0.45$ ; at  $1.65\mu m$ :  $0.45$ ; at  $2.1\mu m$ :  $0.45$ ; at  $3.15\mu m$ :  $0.39$ ; at  $3.95\mu m$ :  $0.33$ , and at  $4.64\mu m$ :  $0.41$ . Our pre-eclipse data were obtained 591 days before our first contact observation, when V was slightly brighter than average. In the Backman et al. data, pre-eclipse IR magnitudes were obtained over a time span of 916 days ( $J=1.77$ ) to 263 days ( $J=1.81$ ) prior to then first contact, although simultaneous V magnitudes were not available for comparison. We infer that effects of the cold disk material impact the infrared spectrum prior to optical first contact, consistent with neutral potassium 7699A equivalent width increases that were detected weeks prior to V band first contact (Leadbeater and Stencel, 2010).

The  $\sim 0.1$  magnitude optical photometric variations out of eclipse and during totality are well-known, and are seen to persist during the 2010 eclipse. During autumn 2010, those variations were particularly well seen, with a local maxima at RJD 55467 and 55550 (Figure 2). The flux *ratio* of the local maximum at RJD 55647 to the local minimum that follows at RJD 55499 is 1.18 at

1.1  $\mu\text{m}$ , 1.24 at 1.65  $\mu\text{m}$ , 1.27 at 2.1  $\mu\text{m}$ , 1.22 at 3.15  $\mu\text{m}$ , 1.29 at 3.95  $\mu\text{m}$  and 1.39 at 4.65  $\mu\text{m}$ . UBVRI magnitude changes reported by Hopkins et al. over this same interval include  $\Delta U = 0.10$ ,  $\Delta B = 0.09$  and  $\Delta V = 0.08$ ,  $\Delta R = 0.06$  and  $\Delta I = 0.02$  magnitudes. As small changes in magnitude are close to ratio quantities, the flux variation seems to be *minimum* in the *red*, but *larger* in the *near-UV* and *near-IR*. The lack of any gross phase lags suggests a coherent phenomenon where a combination of temperature and opacity rules the amplitude. While these variations have been attributed to F star pulsation, whether the overall brightness variations are due to pulsational *hotspots* on the F star, and/or *changes* in the disk material density and opacity remains to be determined.

### 2.1.2. Line variations

In addition to continuum variation largely due to obscuration of the F star by the opaque disk, there are numerous hydrogen absorption lines and as previously noted, plus persistent 4.05 $\mu\text{m}$  Br  $\alpha$  emission (Backman, Simon and Hinkle, 1985). Eclipse-phased differences among these line strengths were noted, as follows: Br  $\alpha$  remains in emission and essentially unchanged in overall strength (equivalent width) throughout eclipse. In contrast, 2.16 $\mu\text{m}$  Br  $\gamma$  absorption strength shows a decrease as eclipse begins, although after mid-eclipse, the strength mimics V band light variations - Figure 3. This behavior is consistent with statements by Backman et al. and earlier researchers that the hydrogen does not clearly associate with either component in the  $\epsilon$  Aurigae binary. Previously mentioned Spitzer IRS data also show hydrogen recombination emission, H $\alpha$  at 12.4 $\mu\text{m}$  (Stencel, 2007). Thus, it is reasonable to infer that the infrared spectrum would be dominated by nebular recombination lines, except for the dominance of the F star absorption spectrum when out of eclipse. We tested this idea by normalizing and differencing the pre-eclipse spectrum (2008 Jan 27) with the mid-eclipse spectrum (2010 Aug 24), both obtained with narrow slits. Line depths are less at mid-eclipse, and the scaled difference in the Brackett series is a clear set of weak emission lines (Figure 4). This is consistent with the reduced absorption equivalent width of Br $\gamma$  (Figure 2a), and evidence for core emission reported in 0.65 $\mu\text{m}$  H $\alpha$  at mid-eclipse. This strongly suggests an extended low density distribution of ionized material between the components, the likes of which could be confirmed by interferometric spectroscopy (e.g. the VEGA instrument at CHARA Array - D.Mourard, private communication) and/or high resolution mid-IR imaging.

### 2.1.3. Appearance of the He I 10830 $\text{\AA}$ line at mid-eclipse

Unexpectedly, we witnessed the appearance of strong He I line absorption at 1.083 $\mu\text{m}$  in our closest to mid-eclipse spectrum (2010 Aug 24) - Figure 1b. The extra absorption converted an 0.2 $\text{\AA}$  equivalent width photospheric line prior to RJD 55,250 (possibly stellar He I, 250m $\text{\AA}$  is consistent with normal B5V stars, Leone et al. 1995) into a feature as large as 5 $\text{\AA}$  in equivalent width during/after mid-eclipse. The excess absorption persisted for months thereafter [4.7 $\text{\AA}$  on RJD

55,432; 3.3Å on 55,467; 3.1Å on 55,499, and 2.2Å on 55,513], with the excess absorption finally disappearing in the 55,537 (2010 Dec 07) spectrum (0.6Å, and 0.2Å on 55,569). The velocity resolution with SpeX as used is only 70 km/sec, which is less than the anticipated motions in the  $\epsilon$  Aurigae system ( $\pm 30$  km/sec). Our observations are merely consistent with the absorption originating in either component (more likely the B star), as opposed to a high speed stream, for instance. Higher resolution spectra around the orbit could help secure the small but persistent absorption's point of origin.

The He I 1.083 $\mu$ m line arises from the ground state of the metastable triplet with components at 1.082909 $\mu$ m, 1.083025 $\mu$ m and 1.083034 $\mu$ m, in that order of laboratory intensity and from a lower level that is 19.82 eV above ground. Thus, whether radiatively pumped or collisionally excited, He I 1.083 $\mu$ m represents plasma well in excess of 25,000K, and up to 230,000K if in thermal equilibrium (Zarro and Zirin, 1986; Sanz-Forcada and Dupree, 2008). This heated region could represent the presence of a compact object, or more likely, accretion onto the hidden star inside the disk. The He II line at 1.0123 $\mu$ m was not detected, neither was the He I singlet at 2.06 $\mu$ m, and the Ca II triplet near 0.85 $\mu$ m remained strong and unchanging. Ancillary lines that appeared briefly during this interval included 15950Å (Mg I) and 16896Å (Fe I?). As a side note, during the analysis of the He I 1.083 $\mu$ m line, we also noticed that 1.1289 $\mu$ m Pa- $\beta$  showed transient emission characteristics in the 2009 Nov.4 and 2009 Dec.1 spectra, and reports of transient emission in He I 0.6678 $\mu$ m (singlet) have been noted elsewhere.

The presence of He I during mid-eclipse provides constraints on the central star characteristics. We can estimate the gas density in the central part of the disk by noting the column density from CO (Hinkle and Simon 1987):  $3 \times 10^{20} \text{ cm}^{-2}$ , that implies  $n_H$  is  $\sim 1.5 \times 10^{24} \text{ cm}^{-2}$ , and the latter is consistent with lack of soft Xrays (Wolk et al. 2010) who report that  $n_H \geq 1.25 \times 10^{24} \text{ cm}^{-2}$ . The column through the 3.8AU radius disk implies a number density approximately  $2.6 \times 10^{10} \text{ cm}^{-3}$ , which is similar to the density deduced by KSM for the HIPPARCOS distance of 625 pc. Using the relative orbital speed reported in KSM and Hack and Selvelli (1979), we deduce a He I zone width close to 1 AU. Then it is straightforward to compute the Stromgren sphere dimension for upper main sequence stars, using tabulated mass, radius and effective temperatures, and the He recombination rate of  $1 \times 10^{-15} \text{ cm}^3 \text{ s}^{-1}$  for 20,000K and the number of ionizing photons shortward of 505Å. We find that a B0V star can create a 1.3AU Stromgren sphere, while a B5V star can manage only 0.05AU. However, HHS and Howell, Hoard and Stencel (2011) provided evidence that the central star more nearly resembles a B5V type photosphere, but with the superposition of UV nebular emission features. To achieve a larger Stromgren sphere with the B5V star, we can add the effect of accretion, and boost the luminosity from accretion by  $G M_* (dM/dt) / R_*$ . With  $dM/dt = 1 \times 10^{-6} M_\odot \text{ yr}^{-1}$  ( $\sim 1$  earth mass per year) the Stromgren sphere for the B5V star with accretion grows to 0.85AU, close to the observed zone size, although the estimated thermal gain from accretion is  $1 \times 10^7 \text{ K}$ , and we assumed this results only in ionizing 505Å photons. A more detailed analysis is in preparation (see Pequette, Stencel and Whitney, 2011).

#### 2.1.4. Re-appearance of molecular CO

As indicated in Table 1, observations 32 days after nominal mid-eclipse (RJD 55,400) did not detect any CO (2-0) near  $2.3 \mu\text{m}$ , while the next epoch, 67 days after mid-eclipse, did so. Figure 1c shows the re-appearance of CO (2-0) bands, which have strengthened in every subsequent observation, and can be anticipated to persist past the end of optical eclipse (4th contact). As noted by Takeuti (2011), the outer disk rotation period is approximately 3 years, assuming a 5.9 solar mass central star. In unperturbed Keplerian motion, the 35 day time interval noted here translates to  $\sim 0.1\text{AU}$ , or a remarkably small 1 percent of the disk circumference, over which CO is sublimated from, or radiatively driven away from, disk particles. For lack of more precise terminology, we will refer to this as a *terminator shock* where F star radiation is on the rise. The significance of re-appearance of molecular CO lies in the gas to dust constraint it provides in understanding the disk structure and evolution. If CO is a result of comet-like sublimation of icy surfaces of solids in the disk, then searches at other wavelengths may succeed in detecting related molecules like  $\text{CO}_2$ ,  $\text{H}_2\text{O}$  and OH, for *years* after eclipse. While SpeX resolution was too low to resolve individual lines, Gemini North IR Spectrometer (GNIRS, T. Geballe, private communication) was used to obtain observations at high dispersion on 2011 Jan 04, and these confirmed the presence of CO (2-0) and (3-1) components at intensities comparable to that reported by Hinkle and Simon (1987).

## 2.2. Spitzer/IRAC

The IRAC imager (Fazio et al. 2004) onboard the Spitzer Space Telescope (Werner et al. 2004) has, in warm mission phase, two operational channels that provide simultaneous  $5.2 \text{ arcmin}$  by  $5.2 \text{ arcmin}$  images at  $3.6 \pm 0.3$  and  $4.5 \pm 0.5 \mu\text{m}$ . The goal of this series of measurements was to provide a well-calibrated but independent means of assessing the SED contribution of the cold disk relative to the F star continuum, and to seek evidence for disk temperature increase as post eclipse phases begin to present themselves. A very clever strategy to avoid bright object saturation but retain photometric precision was invented by Steve Howell, and was used to place the star image at the intersection of pixels. In this way we were able to obtain a series of photometric measurements during the semi-annual observing windows since early 2009, as detailed in Table 3. Donald Hoard re-did the photometric extractions using data processing and photometry procedures identical to that described in HHS. All uncertainties in the table below are random (scatter) only. They do not include the systematic uncertainty contributions.

We note the IRAC continuum flux decline in ratio terms, between pre-eclipse (2009 April) and totality (2010 March), were [totality/pre-eclipse], at  $3.6\mu\text{m}$ : 0.64, and at  $4.5\mu\text{m}$ : 0.60, which are somewhat less than flux decline ratios reported by Backman et al. (1984), namely at L band:  $0.52 \pm 0.06$  and at M band:  $0.54 \pm 0.07$ . These are larger than the SpeX results comparing 2009 Sep and 2010 Mar fluxes, at  $3.15\mu\text{m}$ : 0.54 and at  $3.95\mu\text{m}$ : 0.56. Calibration issues aside, we note that SpeX fluxes in 2009 Jan (when  $V = 3.00$ ) were 10-15 percent higher than during 2008

Jan (when  $V = 2.99$ ). During 2009 April when the IRAC baseline was obtained, the star was brightening quickly, and this could account for the differences. Clearly, short-term variations must be monitored to determine changes among eclipse depths. In addition, spectral features intrinsic to the IRAC bands could play a role in these differences. We note that the in-eclipse variations are small, just a few percent, compared those of the optical light which are of order 10 percent. However, the temporal coverage is too limited to make a strong statement.

The externally-heated disk model (Takeuti 2011) suggests that as eclipse progresses, higher temperature facets of the disk ought to rotate into view. Comparing IRAC measurements before and after mid-eclipse, we find small increases of 4 and 2 Jy in the respective channels. Further observations were obtained in 2011 spring to confirm this trend. During egress, V band brightened by 0.4 magnitudes (44 percent) between 2010 Nov 22 and 2011 Apr 12. Meanwhile, IRAC fluxes rose by less: 7.7 Jy (17 percent) and 8.3 Jy (25 percent), respectively, suggesting a second, uneclipsed source of flux is present at those wavelengths (the heated disk). The 2011 April 12 (29) data shows recovery of flux from totality (2010 Nov), in the sense of flux ratios [egress/totality] at  $3.6\mu\text{m}$ : 1.18 (1.24), and at  $4.5\mu\text{m}$ : 1.25 (1.40), which is less change than the V magnitude change (1.44).

Figure 5 plots IRAC channel 1 and 2 flux predictions. Pre-eclipse, we observed IRAC1 and 2 flux densities of  $66.2 \pm 3.0$  and  $52.9 \pm 2.4$  Jy. Predictions from this simulation for heated disks during eclipse are 44.0 and 33.0 Jy (750 K disk) and 57.3 and 47.3 Jy (1000 K disk). Assuming non-systematic uncertainties smaller than 5 percent (consistent with our first DDT observations), we have a sensitive means for diagnosing disk temperature variation during the balance of eclipse, when heated portions of the disk will rotate into view. The 2010 spring ( $V=3.82$ ) and 2010 fall ( $V=3.76$ ) values seem to indicate a disk temperature closer to 700K than the 550K implied by pre-eclipse observations studied by HHS. A broader-band look at the mid-IR SED contributions is detailed below.

### 2.3. BASS

Additional observations were made with BASS, The Aerospace Corporation’s Broadband Array Spectrograph System (Hanner et al. 1994), which spans the 2-14  $\mu\text{m}$  wavelength region using two 58 element block impurity band linear arrays that simulataneously observe all spectral elements. Table 4 lists the observations made, with all of the observations conducted at IRTF, except for 2010 Feb 12 which was conducted at AEOS atop Haleakela, HI. The calibrations and telluric corrections are similar to those described previously with SpeX, within 3 percent uncertainties.

A similar behavior in attenuation of the F star continuum with wavelength is observed as eclipse progresses, with a flux ratio at 11.6  $\mu\text{m}$  of  $1.90 \pm 0.07$  (2009 Jul.14 and 2010 Mar.04), that compares favorably to the N band ratio of  $1.75 \pm 0.09$  reported by Backman et al. (1984). During the course of BASS observations, little deviation from a blackbody continuum was observed, that is, no evidence for any strong silicate or carbon-related solid state features at the usual mid-

infrared wavelengths (Figure 6). However, the longest wavelengths do show departure from a 7500K blackbody curve, consistent with the presence of a second source with a temperature of order 500K or higher. Further observations are planned to confirm this trend.

#### 2.4. MIRSI

The Mid-Infrared Spectrometer and Imager (MIRSI) is a mid-IR filter or CVF imager and low resolution spectrometer that operates in the 8-14 and 18-26  $\mu\text{m}$  bands and optimized for the IRTF (Kassis, et al. 2008). Two epochs of pre-eclipse observations were obtained in 2007 and 2008, as described in Tables 5 and 6, with Capella used as the primary comparison star. The V band magnitudes reported for those pre-eclipse dates was 3.04 and 3.05 respectively. Adopted Capella monochromatic magnitudes and flux densities are: K = -1.83, 3480 Jy; L = -1.89, 1420 Jy; M = -1.95, 982 Jy; N = -1.93, 235 Jy; Q = -2.03, 67 Jy (Persei et al. 2004; Tokunaga and Vacca 2004). We will compare these observations with MIRAC and TNTCAM data in the next sections.

#### 2.5. MIRAC

The Mid-Infrared Array Camera, MIRAC (Hoffmann et al. 1998), originally was built around a 128x128 Si:As BIB array that is sensitive to the 5-20  $\mu\text{m}$  region. The current configuration uses a 256x256 array and is capable of both photometric imaging and low/moderate resolution spectroscopy. Observations were conducted at the Fred L. Whipple Observatory 6 meter MMTO during 2010, as described in Tables 7 and 8. Capella was used as the primary comparison star. The photometric measurements will be compared with MIRSI and TNTCAM in the next section. The spectroscopic results indicate no significant changes in the mid-IR spectrum between early and later phases of totality, consistent with BASS results mentioned above. In both cases, the continuum appears smooth and devoid of any strong 10 micron silicate features at these phases.

#### 2.6. TNTCAM

Denver University’s *Ten and Twenty Micron Camera* [TNTCAM] similarly was constructed around a Rockwell 128x128 Si:As BIB array (Klebe, et al. 1996), and was used for mid-infrared imaging at the Wyoming Infrared Observatory (WIRO, 2.4 meter) and the Mt.Lemmon Observing Facility (MLOF, 60 inch) during the 1990s, at a mid-point between the 1983 and 2010 primary eclipses - suggested by Sheffer and Lambert (1999) to be close to secondary minimum. A newer solution by Chadima et al. (2010) gives 2000 May as the time of secondary minimum. In either event, the decade of the 1990s should have presented the heated face of the disk toward earth.

The observing teams at WIRO and MLOF included Denver astronomers Michelle Creech-

Eakman, Mary Dahm, Matti Jalakas, Dimitri Klebe, Donald Neff and Robert Stencel, plus support personnel from Wyoming (David Ciardi) and Mt.Lemmon (Drs. Mason and Williams). Observations obtained in those times are listed in Table 9. These secondary minimum observations occurred during a period when V band was reported to average  $3.01 \pm 0.03$ . Capella once again served as the primary comparison star, leading to the magnitudes and fluxes reported in Table 10. Analysis of the frames indicates that the mid-IR was  $\sim 50$  percent brighter during the mid-1990s than it was preceding the latest eclipse in 2007-2008 (MIRSI) - see Figure 7, indicative of the hotter face of the disk being oriented toward the observer during superior conjunction in the mid-1990s, in accordance with the model by Takeuti (1986, 2011). For completeness, we add published data obtained during this same timeframe, with the Midcourse Space Experiment (MSX: Egan and Price, 1994), and with groundbased JHKLM photometry reported by Taranova and Shenavrin (2001). These observations show that the infrared spectrum of epsilon Aurigae was a factor 2-3 brighter during secondary minimum, supportive of the model with an externally heated disk facing earth, as proposed by Takeuti (1986, 2011).

### 3. Results

By means of a variety of infrared observations during the 2010 eclipse, we refined and solidified the following results and interpretations concerning the nature of epsilon Aurigae, some of which were introduced by researchers cited herein during the 1983 eclipse:

(1) The IR eclipse depths during 2010 appear similar to that observed during the most recent (1983) eclipse (Backman et al. 1984), indicating relative stability of the objects involved over that timeframe. Spectral line profile changes indicate that the disk is embedded in a hydrogen recombination region (Hack and Selvelli, 1979);

(2) Molecular CO absorption returned 57 days after nominal mid-eclipse (RJD 55,400), although it was not present at mid-eclipse plus 34 days narrowing the association with disk regions to a narrow terminator shock where external radiation from the F star begins to affect the disk (Hinkle and Simon 1987, Takeuti, 1986);

(3) The newly found appearance of excess He I 10830Å absorption associated with mid-eclipse and  $\sim 90$  days thereafter is strongly suggestive of an accretion source embedded in the disk and consistent with a mid B main sequence object, as indicated by SED analysis (Hoard, Howell and Stencel 2010);

(4) The lack of solid state features in BASS and MIRAC spectra, to date, suggests the dominance of micron-sized or larger particles in the disk, to account for the broadband opacities;

(5) Comparison of pre- and in-eclipse data, along with superior and inferior conjunction data, appears to demonstrate differential heating of the disk due to the presence of the nearby F star, resulting in a 550K surface facing the observer during primary eclipse, and a  $\sim$ 1100K surface facing the observer during secondary minimum. Further mid and far-IR observations can help constrain the heat capacity of the disk material, leading to more comprehensive disk models than presently available. Efforts should be made to image the disk out of eclipse with mid-IR interferometry during the coming decade, as the system approaches quadrature.

This work was supported in part by the bequest of William Herschel Womble in support of astronomy at the University of Denver, by NSF grants AST 97-24506 and AST 10-16678, and JPL RSA 1414715 to the University of Denver, by NASA ADP grant NNX09AC73G to the University of Cincinnati, and by The Aerospace Corporation's Independent Research and Development Program. Observations reported here were obtained in part as Visiting Astronomers at the Infrared Telescope Facility, which is operated by the University of Hawaii under Cooperative Agreement NNX-08AE38A with the National Aeronautics and Space Administration, Science Mission Directorate, Planetary Astronomy Program. Observations reported here were obtained in part at the MMT Observatory, a joint facility of the Smithsonian Institution and the University of Arizona. Observations were also obtained in part at the University of Wyoming's Infrared Observatory (WIRO), involving access for which we are grateful. The first author thanks Dana Backman for the encouragement to obtain mid-IR data during the mid-1990s, and the many observers involved in those and all the data reported here. We also thank Jeff Hopkins, Brian McCandless, Thomas Rutherford and the AAVSO for access to their visual observation records.

*Facilities:* IRTF (SpeX), MMT (MIRAC4), Spitzer (IRAC).

## REFERENCES

- Backman, D., Becklin, E., Cruikshank, D., Joyce, R., Simon, T. and Tokunaga, A. 1984 ApJ, 284, 799.
- Backman, D. and Gillett, F., 1985 ApJ, 299, L99.
- Backman, D., Simon, T. and Hinkle, K. 1985 PASP, 97, 1163.
- Chadima, P., Harmanec, P., Yang, S., Bennett, P., Boi, H., Rudjak, D., Sudar, D., koda, P., lechta, M., Wolf, M., Lehk, M. and Dubovsk, P., 2010, IBVS 5937.
- Cushing, M., Vacca, W. and Rayner, J. 2004 PASP, 116, 362 (Spextool).
- Egan, M. and Price, S. 1996 AJ, 112, 2862.
- Fazio, G. *et al.* 2004 ApJS, 154, 10.

- Guinan, E. and Dewarf, L. 2002, in C. A. Tout & W. van Hamme, editors, in *Exotic Stars as Challenges to Evolution* A.S.P. Conf. Ser. vol. 279, p. 121.
- Hack, M. and Selvelli, P. 1979 *Astron.Astrophys.*, 75, 316.
- Hanner, M., Lynch, D. and Russell, R. 1994 *ApJ*, 425, 274.
- Hinkle, K. and Simon, T., 1987 *ApJ*, 315, 296.
- Hoard, D., Howell, S. and Stencel, R., 2010 *ApJ*, 714, 549 [HHS].
- Hoffmann, W. F., Hora, J. L., Fazio, G. G., Deutsch, L. K., & Dayal, A. 1998, in *Infrared Astronomical Instrumentation*, ed. A. M. Fowler, *Proc. SPIE* 3354, 647-658.
- Hopkins, J. and Stencel, R. 2011, *AAS*, 217, 257.01.
- Howell, S., Hoard, D. and Stencel, R., 2011, *AAS*, 217, 257.07.
- Huang, S.-S. 1965, *ApJ*, 141, 976.
- Kassis, M., Adams, J., Hora, J., Deutsch, L. and Tollestrup, E. 2008, *PASP*, 120, 127.
- Klebe, D., Dahm, M. and Stencel, R. 1996 in *Polarimetry of the interstellar medium*, *Astronomical Society of the Pacific Conference Series*; eds. W. Roberge and D. Whittet, Vol. 97, p.79.
- Kloppenborg, B., Stencel, R., Monnier, J.D., Schaefer, G., Zhao, M., Baron, F., McAlister, H. A., ten Brummelaar, T. A., Che, X., Farrington, C.D., Pedretti, E., Sallave-Goldfinger, P.J., Sturmman, J., Sturmman, L., Thureau, N., Turner, N., and Carroll, S., 2010, *Nature (Letters)*, 464, 870 [KSM].
- Lambert, D. and Sawyer, S. 1986 *PASP*, 98, 389.
- Leadbeater, R. and Stencel, R. 2010, <http://arxiv.org/abs/1003.3617> .
- Leone, F., Lanzafame, A.C. and Pasquini, L. 1995, *Å*, 293, 457.
- Persi, P., Ferrari-Toniolo, M., Ranieri, M., Marenzi, A. and Shivanandan, K. 1990 *Astron.Astrophys.*, 237, 153.
- Pequette, N., Stencel, R. and Whitney, B. 2011 *AAS*, 218, 225.05 .
- Rayner, J., Toomey, D., Onaka, P., Denault, A., Stahlberger, W., Vacca, W., Cushing, M., and Wang, S. 2003 *PASP*, 115, 362.
- Sanz-Forcada, J. and Dupree, A. 2008 *Astron.Astrophys.*, 488, 715.
- Sheffer, Y. and Lambert, D. 1999, *PASP*, 111, 829.
- Stencel, R. 2007 in *Binary Stars as Critical Tools & Tests in Contemporary Astrophysics*, *Proceedings of IAU Symposium 240*. Edited by W.I. Hartkopf, E.F. Guinan and P. Harmanec. Cambridge: Cambridge University Press, pp.202-204.
- Stencel, R. 2010, <http://arxiv.org/pdf/1005.3738> .
- Takeuti, M. 1986 *Astrophys. Space Sci.* 121, 127.
- Takeuti, M. 2011 *PASJ*, 63, 325.

- Taranova, O. and Shenavrin, V. 2001 *Astron.Lett.*, 27, 338.
- Tokunaga, A. and Vacca, W. 2005 *PASP*, 117, 421.
- Vacca, W., Cushing, M. and Rayner, J. 2003 *PASP*, 115, 389.
- Werner, M. *et al.* 2004 *ApJS*, 154, 1.
- Wolk, S., Pillitteri, I., Guinan, E. and Stencel, R. 2010 *AJ*, 140: 595.
- Zarro, D. and Zirin, H. 1986 *ApJ*, 304,365.

Table 1. SpeX observations, SXD and LXD, 0.8 to 4.6  $\mu\text{m}$ .

J.D.	Date	Observers	Notes
2,454,493	2008 Jan.27	JTR et al.	V=3.00, slit 0.5, CO absent
2,454,842	2009 Jan.10	RES/BKK	V=2.99, slit 0.3, CO absent, LXD only
2,455,084	2009 Sep.10	JTR et al.	V = 3.12, slit 0.5, CO absent
2,455,140	2009 Nov.04	JTR et al.	V=3.43, slit 0.5, CO absent
2,455,167	2009 Dec.01	MS et al.	V=3.53, slit 0.8, CO absent
2,455,250	2010 Feb.24	RES/BKK	V=3.77, slit 0.8, CO absent
2,455,432	2010 Aug.24	RES/BKK	V=3.73, slit 0.3, CO absent, He present
2,455,467	2010 Sep.27	RES/BKK	V=3.69, slit 0.3, CO, He present
2,455,494	2010 Oct.24	MS et al.	V=3.72, slit 0.8, CO, He present
2,455,499	2010 Oct.29	RES/BKK	V=3.74, slit 0.3, CO, He present
2,455,513	2010 Nov.12	RES/BKK	V=3.76, slit 0.3, CO, He present, cirrus
2,455,537	2010 Dec.6	RES/BKK	V=3.72, slit 0.3, CO present
2,455,569	2011 Jan.6	RES/BKK	V=3.76, slit 0.3, CO present
2,455,624	2011 Mar.4	MS et al.	V=3.72, slit 0.8, CO present, clouds
2,455,649	2011 Mar.29	JTR et al.	V=3.55, slit 0.5, CO present

Table 2. SpeX + IRTF monochromatic fluxes [ $\lambda f_\lambda$  per  $10^{-10}$  W m $^{-2}$ ] at selected continuum wavelengths ( $\mu\text{m}$ ).

J.D.	Date	1.1	1.65	2.1	3.15	3.95	4.64	Notes
2,454,493	2008Jan.27	9.46	4.77	2.75	1.04	0.60	0.41	Pre
2,454,842	2009Jan.10	–	–	2.88	1.17	0.69	–	
2,455,084	2009Sep.10	7.77	3.97	2.31	0.81	0.46	0.31	I
2,455,140	2009Nov.04	6.63	3.38	1.95	0.74	0.40	0.30	
2,455,167	2009Dec.01	5.81	2.95	1.70	0.64	0.35	0.23	
2,455,250	2010Feb.23	4.18	2.11	1.25	0.46	0.26	–	II
2,455,432	2010Aug.24	4.79	2.45	1.40	0.50	0.27	0.20	Mid
2,455,467	2010Sep.27	5.37	2.75	1.61	0.62	0.33	0.25	
2,455,494	2010Oct.24	4.89	2.51	1.45	0.53	0.30	0.21	
2,455,499	2010Oct.29	4.57	2.22	1.27	0.34	0.17	0.12	
2,455,513	2010Nov.12	1.75:	0.89:	0.48:	0.19:	0.11:	0.07:	cirrus
2,455,537	2010Dec.06	4.91	2.48	1.46	0.58	0.32	0.21	
2,455,569	2011Jan.07	5.39	2.75	1.57	0.58	0.32	0.21	
2,455,649	2011Mar.29	12.5	6.08	3.47	1.26	0.71	0.44	III

Table 3. IRAC observations.

J.D. Notes	Date	Flux[Jy]	
		3.6 $\mu$ m	4.5 $\mu$ m
2,454,947 V = 3.02	2009 Apr.26	66.3 $\pm$ 0.05	52.9 $\pm$ 1.4
2,455,283 V = 3.73	2010 Mar.28	42.3 $\pm$ 0.6	31.9 $\pm$ 0.6
2,455,305 V = 3.82	2010 Apr.19a	42.3 $\pm$ 0.2	31.8 $\pm$ 0.3
2,455,305 V = 3.82	2010 Apr.19b	42.5 $\pm$ 0.2	31.8 $\pm$ 0.2
2,455,500 V = 3.76	2010 Oct.30a	46.1 $\pm$ 0.8	33.6 $\pm$ 0.2
2,455,500 V = 3.76	2010 Oct.30b	46.4 $\pm$ 0.8	33.6 $\pm$ 0.2
2,455,523 V = 3.76	2010 Nov.22a	45.5 $\pm$ 0.6	32.9 $\pm$ 0.2
2,455,523 V = 3.76	2010 Nov.22b	45.7 $\pm$ 0.6	32.9 $\pm$ 0.2
2,455,664 V = 3.40	2011 Apr.12	53.3 $\pm$ 1.6	41.2 $\pm$ 1.1
2,455,680 V = 3.35	2011 Apr.29	58.9 $\pm$ 1.2	45.9 $\pm$ 0.2

Table 4. BASS observations.

J.D.	Date	Observers	$\lambda F_{11.6\mu}$ W m $^{-2}$
2,454,082	2006 Dec.11	MS/RR/DL	3.774E-12
2,454,713	2008 Sep.03	MS/RR/DL	3.254E-12
2,455,027	2009 Jul.14	MS/RR/DL	3.381E-12
2,455,165	2009 Nov.29	MS/RR/DL	2.182E-12
2,455,209	2010 Feb.12	MS/RR/DL	1.834E-12
2,455,260	2010 Mar.04	MS/RR/DL	1.780E-12
2,455,493	2010 Oct.23	MS/RR/DL	1.844E-12
2,455,769	2011 Jul.29	MS/RR/DL	4.0E-12

Table 5. MIRSI + IRTF observations.

J.D.	Date	Observers	Notes
2,454,164	2007 Mar.04	GO/YPF	10 $\mu\text{m}$ imaging
2,454,484	2008 Jan.17	GO/YPF	20 $\mu\text{m}$ imaging
2,455,260	2010 Mar.03	MS/RR/DL	10 $\mu\text{m}$ imaging

Table 6. MIRSI observations, 2007 Mar.04,  $V=3.04$ .

$\lambda$	$\epsilon$ Aur - $\alpha$ Aur	$\pm$	$m(\epsilon$ Aur)	$\epsilon$ Aur[Jy]
7.7	3.25	0.06	1.31	19
9.8	3.37	0.05	1.44	11
12.5	2.87	0.08	0.91	11
MIRSI	2008 Jan.17	$V=3.05$		
17.2	2.90	0.06	0.90	6
17.9	2.81	0.05	0.80	6
18.4	2.70	0.10	0.69	6
20.8	2.99	0.03	0.96	4
24.8	2.63	0.08	0.58	4
MIRSI	2010 Mar. 03	$V=3.77$		
4.9	3.69	0.03	1.74	33
7.7	3.62	0.04	1.68	14
8.7	3.62	0.03	1.68	11
9.8	3.60	0.03	1.67	9
11.6	3.52	0.04	1.59	7
12.5	3.44	0.06	1.51	7

Table 7. MIRAC + MMT0 observations.

J.D.	Date	Observers	Notes
2,455,198	2010 Jan.01	JH/WH/AS	$V=3.67$ , 10 $\mu\text{m}$ silicates absent
2,455,552	2010 Dec.21	RES/PH	$V=3.70$ , 10 $\mu\text{m}$ silicates absent

Table 8. MIRAC + MMT0 observations, 2009 Dec.31,  $V=3.67$ , RJD 55197.

$\lambda$	$\epsilon$ Aur - $\alpha$ Aur	$\pm$	$m(\epsilon$ Aur)	$\epsilon$ Aur[Jy]
2.2	4.16	0.05	2.33	$80 \pm 4$
3.9	4.03	0.07	2.14	$38 \pm 2$
4.7	4.02	0.08	2.07	$26 \pm 2$
8.7	2.71:	0.15	0.78:	10:
9.8	3.39	0.06	1.46	$8 \pm 1$
10.5	3.10	0.11	1.17	$9 \pm 1$
11.8	2.77	0.01	0.82	$6 \pm 1$
12.5	2.43	0.03	0.48	$6 \pm 1$

Table 9. TNTCAM observations.

J.D.	Date	Notes
2,450,026	1995 Nov.05	11 $\mu$ m imaging, WIRO
2,450,101	1996 Jan.19	10, 11 $\mu$ m imaging, WIRO
2,450,145	1996 Mar.03	10, 11 $\mu$ m imaging, WIRO
2,450,187	1996 Apr.14	8-18 $\mu$ m imaging, MLOF
2,450,333	1996 Sep.07	5-18 $\mu$ m imaging, WIRO
2,450,394	1996 Nov.07	5-12 $\mu$ m imaging, WIRO
2,450,426	1996 Dec.09	5-18 $\mu$ m imaging, WIRO

Table 10. Archival and TNTCAM observations near Sec. Min.,  $V=3.02 \pm 0.03$ .

Date	$\lambda$	$\epsilon$ Aur - $\alpha$ Aur	$\pm$	$m(\epsilon$ Aur)	$\epsilon$ Aur[Jy]
1998-2000	1.25 (J)	—	—	—	287±8
(Taranova	1.65 (H)	—	—	—	242±11
et al., 2001)	2.20 (K)	—	—	—	174±5
	3.75 (L)	—	—	—	95±3
	4.7 (M)	—	—	—	54±1
MSX, 1999	4.29	—	—	—	68
(IRSA,)	4.35	—	—	—	72
Vizier)	8.28	—	—	—	24
	12.13	—	—	—	12
	13.5	—	—	—	10
	21.34	—	—	—	5
1995Nov	11.6	2.96	0.28	1.01	13±1
WIRO					
1996Jan	10.3	2.95	0.06	1.02	15±1
WIRO	10.3	2.83	0.06	0.90	17±1
	11.6	2.73	0.12	0.78	15±2
	11.6	2.79	0.10	0.84	14±1
	11.6	2.73	0.10	0.78	15±1
1996Mar	10.3	2.74	0.13	0.81	19±2
WIRO	11.6	2.63	0.14	0.68	17±2
1996Apr22	2.2	3.20	0.05	1.37	193
MLOF*	4.8	2.94	0.05	0.99	61
Mason,	7.8	2.80	0.08	0.86	29
Williams	8.7	2.98	0.08	1.04	19
	9.8	2.86	0.08	0.93	17
	10.3	2.92	0.10	0.99	14
	11.6	2.63	0.10	0.70	16
	12.5	2.63	0.10	0.70	14
1996May	7.8	2.90	0.22	0.96	26±5
MLOF	10.3	2.85	0.17	0.92	17±3
	11.6	2.71	0.18	0.76	16±3
	12.5	2.68	0.15	0.73	13±3

Table 10—Continued

Date	$\lambda$	$\epsilon$ Aur - $\alpha$ Aur	$\pm$	$m(\epsilon$ Aur)	$\epsilon$ Aur[Jy]
1996May29	2.2	3.32	0.05	1.49	172 $\pm$ 9
MLOF*	4.8	3.02	0.05	1.07	56 $\pm$ 3
Mason,	7.8	2.91	0.08	0.97	27 $\pm$ 2
Williams	8.7	2.91	0.08	0.97	20 $\pm$ 2
	9.8	2.80	0.08	0.87	18 $\pm$ 1
	10.3	2.76	0.10	0.83	17 $\pm$ 2
	11.6	2.52	0.10	0.59	17 $\pm$ 2
	12.5	2.53	0.10	0.60	15 $\pm$ 1
1996Sep	4.6	2.98	0.02	1.03	57 $\pm$ 1
WIRO	10.3	2.88	0.05	0.95	16 $\pm$ 1
	11.6	2.79	0.06	0.84	14 $\pm$ 1
	12.5	2.78	0.09	0.83	13 $\pm$ 1
1996Nov	4.6	3.05	0.02	1.10	56 $\pm$ 2
WIRO	4.6	2.85	0.03	0.90	67 $\pm$ 2
	7.8	2.86	0.19	0.92	27 $\pm$ 5
	7.8	2.67	0.04	0.73	32 $\pm$ 1
	10.3	2.79	0.06	0.86	18 $\pm$ 1
	11.6	2.59	0.06	0.64	17 $\pm$ 1
1996Dec	4.6	2.98	0.07	1.03	57 $\pm$ 4
WIRO	10.3	2.61	0.14	0.68	21 $\pm$ 3
	11.6	2.98	0.51	1.03	12 $\pm$ 6

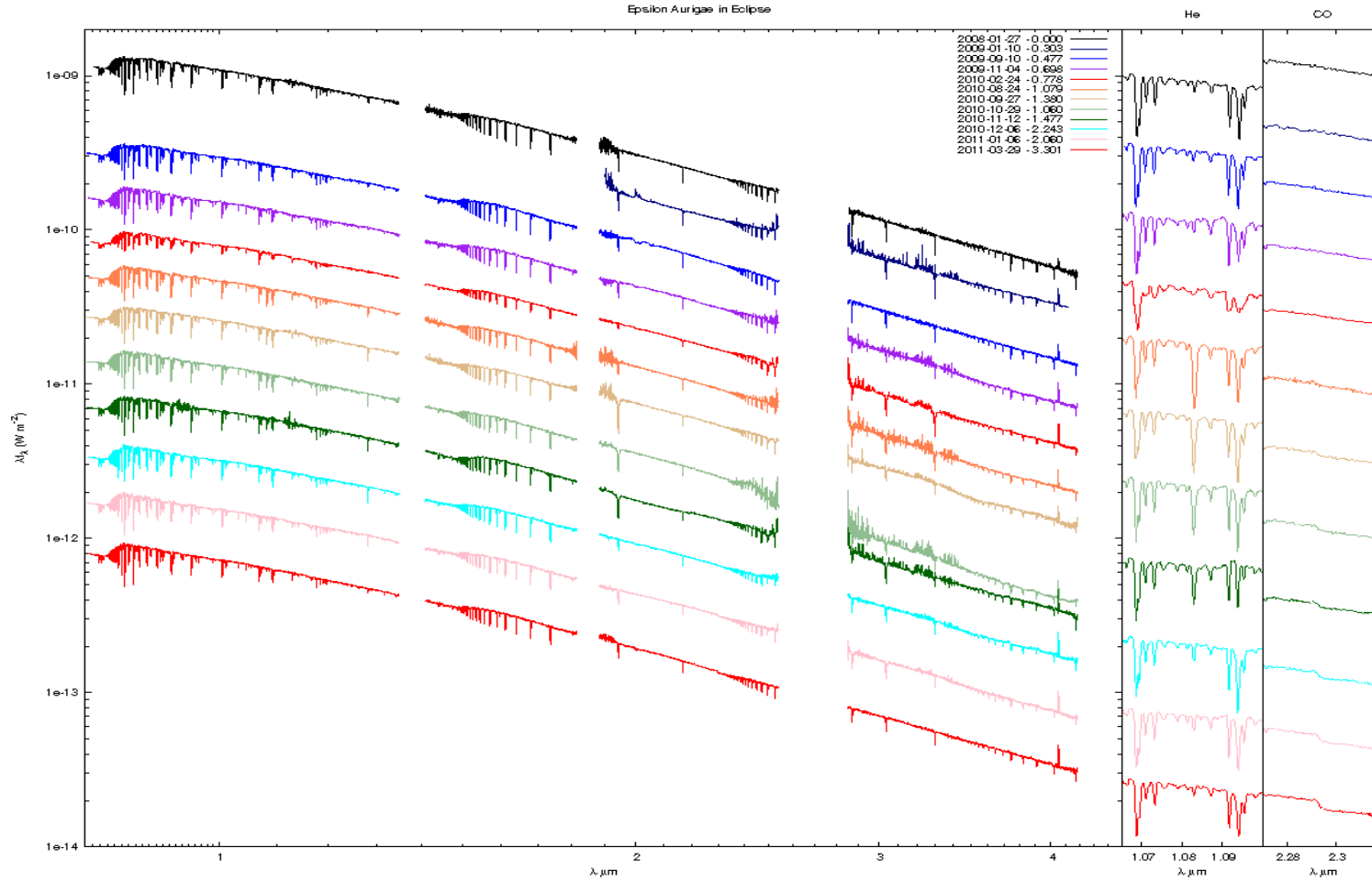


Fig. 1.— The SpeX record of the eclipse of epsilon Aurigae, starting with pre-eclipse data in 2008, ingress (fall 2009), totality (2010). These data reveal continuum and line changes, including transient He I (1.0830 microns, detailed in the first box, right) during mid-eclipse (Aug-Dec 2010), plus 2.29 micron CO absorption appearing after mid-eclipse (second box, far right). For clarity, the continuum levels have been offset by the logarithmic factors next to the date caption list.

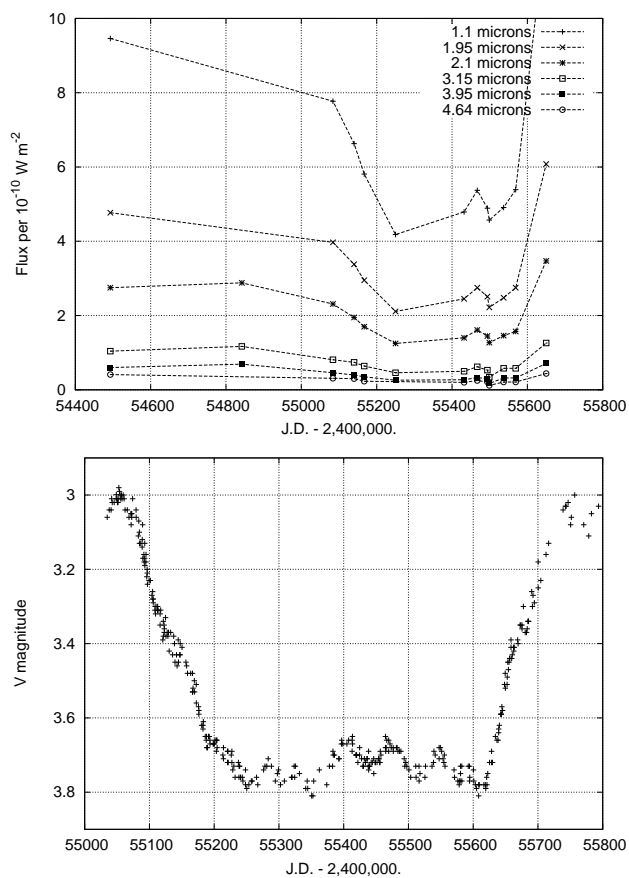


Fig. 2.— SpeX observations of the *continuum* differences at different wavelengths, between local optical light maxima [RJD 55,467 and 55,550] and local minima [55,432 and 55,499], compared with the V band light curve (observer names include J.Hopkins, R.Miles, D.Loughney, C.Hofferber, H.G.Lindberg, Th.Karlsson, E.Guinan, M.Strikis, F.Melillo and others - see Hopkins and Stencel 2011).

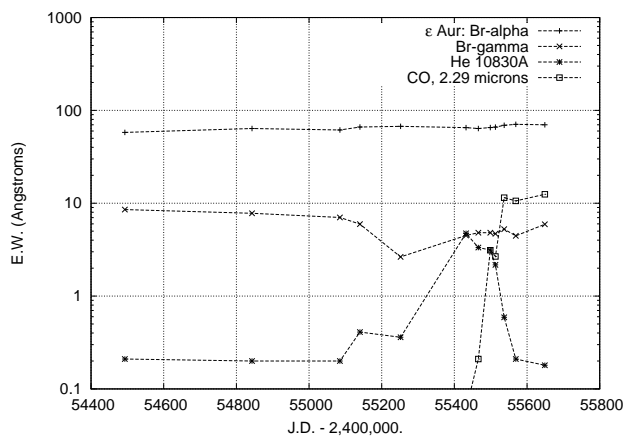


Fig. 3.— SpeX observations of equivalent widths of lines in  $\epsilon$  Aurigae on selected dates.

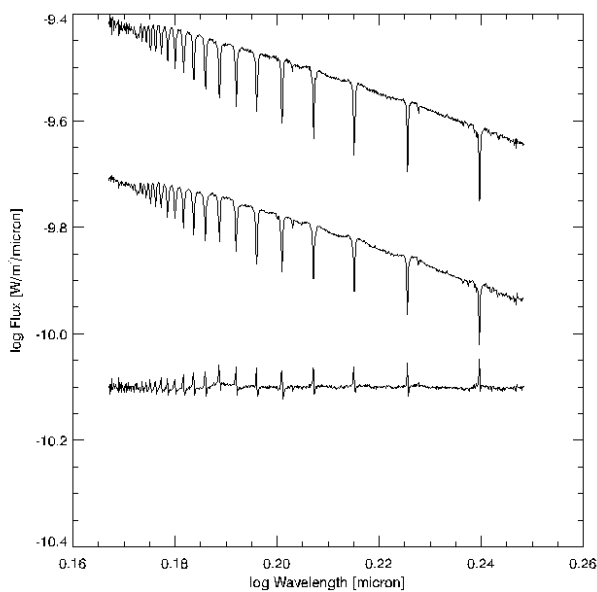


Fig. 4.— SpeX flux distribution and scaled differences of lines approaching the Brackett limit near  $1.5\mu\text{m}$ , pre-eclipse to mid-eclipse, showing the recombination spectrum of extended disk material in  $\epsilon$  Aurigae.

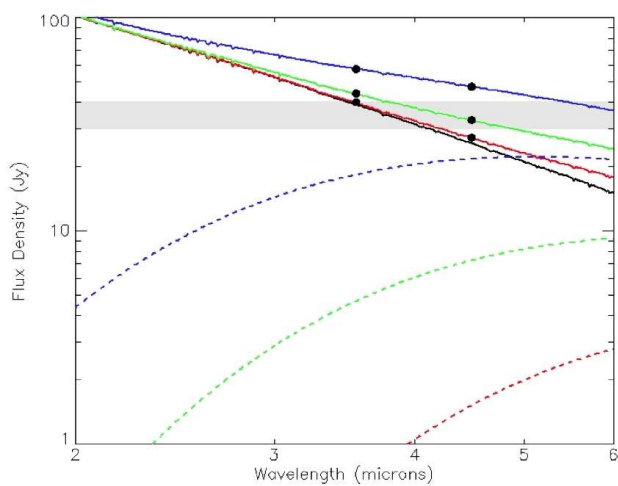


Fig. 5.— A plot of IRAC channels 1 and 2 flux predictions. The dashed lines show (from bottom to top) disk models (as in HHS10) with temperatures of 550 K, 750 K, and 1000 K. The solid lines show (from bottom to top): F star template reduced by 50 percent to account for eclipse, and the sums of the eclipsed F star and the three disk models. See text for details.

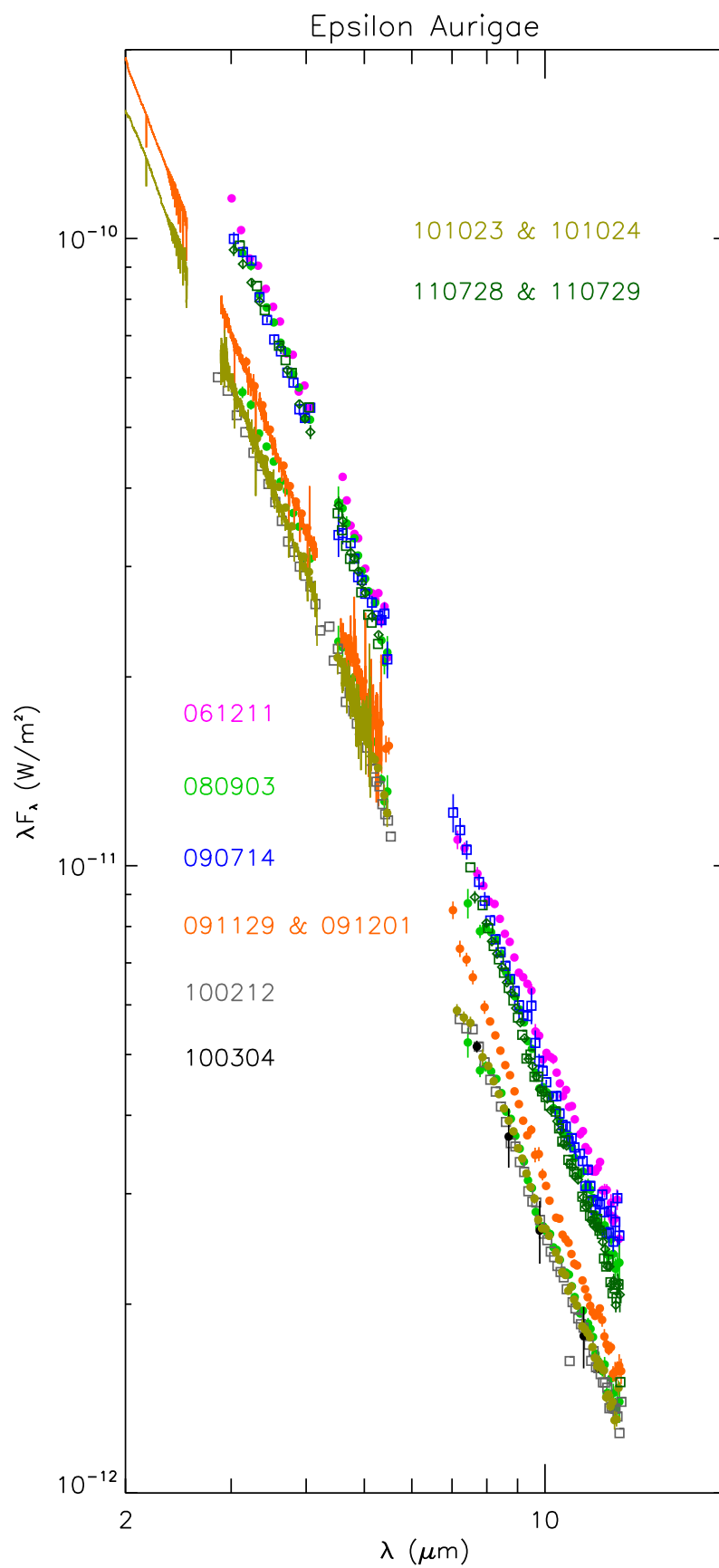


Fig. 6.— BASS observations of  $\epsilon$  Aurigae on selected dates, 2006-2010.

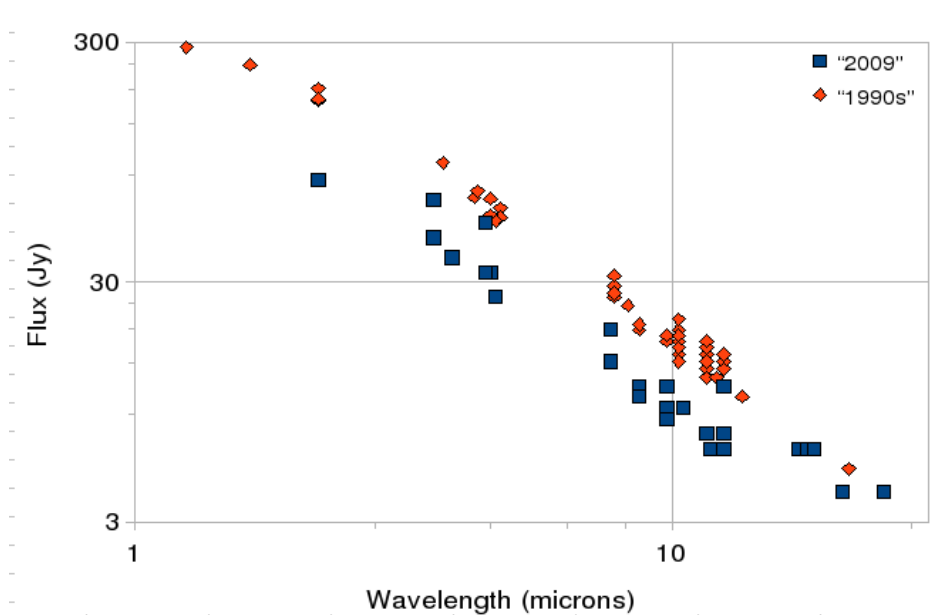


Fig. 7.— Mid-IR observations of  $\epsilon$  Aurigae. The "2009" data refer to MIRSI photometry (obtained in 2007 and 2008, preceding the current eclipse) and IRAC photometry (pre-eclipse), with MIRAC data (obtained in early 2010, during totality). The "1995" data refer to a combination of TNTCAM photometry, along with MSX and ground based photometry published by Taranova and Shenavrin (2001) obtained in 1996-1999, approximately during superior conjunction or secondary minimum). The comparison demonstrates that the disk was distinctly hotter during secondary minimum timeframe (1996) compared with total eclipse (2010).